

# Natural convection in an inclined parallelogram-shaped enclosure containing internal energy source with linearly heated sidewall

Hayder Kraidi Rashid Nasrawi<sup>1</sup>; Mohammed Yousif Jabbar<sup>3</sup>; Salam Hadi Hussain<sup>2</sup>;  
Farooq Hassan Ali<sup>3</sup>

1, Ceramic Engineering Department- College of Materials Engineering- Babylon University - Babylon Province - Iraq.

2, Automobile Engineering Department-College of Engineering/Al-Musayab-Babylon University-Babylon Province - Iraq.

3, Mechanical Engineering Department- College of Engineering- Babylon University - Babylon Province - Iraq.

## Abstract

The main objective of this paper is to study the natural convection flow inside a parallelogram enclosure having uniform internal heat generation. The left inclined wall is linearly heated while the right inclined wall is kept at cold temperature ( $T_c$ ) and top and bottom walls are thermally insulated. Steady state, two-dimensional numerical study is carried out by using the finite volume technique after the equations are put into dimensionless forms. The governing parameters studied are external Rayleigh number, internal Rayleigh number and inclination angle from horizontal axis which are varied from  $10^3 \leq Ra_E \leq 10^6$ ,  $0 \leq Ra_I \leq 10^8$  and  $0^\circ \leq \Phi \leq 45^\circ$ . Air is used as a working fluid with a Prandtl number of 0.71. Efforts are focused on the interaction between the internal Rayleigh number (heat generation) and external Rayleigh number (temperature difference between the sidewalls) for various inclination angles. The accuracy of the numerical method compared with the previous published works shows an excellent agreement. The obtained results show that the maximum heat transfer performance occurs at zero inclination angle and low values of external heating.

**Keywords:** Natural convection; heat generation; linear heating; parallelogram enclosure; finite volume.

## 1. Introduction

The natural convection in enclosures with internal heat generation and linearly heated side wall is relevant to many industrial and environmental applications such as nuclear reactor design, post-accident heat removal in nuclear reactors, geophysics and underground storage of nuclear waste, boilers, energy storage systems and conservation, fire control and chemical, food and metallurgical industries etc. A few researchers dealing with the natural convection in parallelogrammic enclosures are found in literature [1-8]. Most of natural convection studies have been carried out in square, triangle and trapezoidal cavities with linearly heated or cooled side wall(s) or bottom wall(s), [9-13]. Finite element simulation has been performed by Tanmay et al. [9], to investigate the influence of linearly heated sidewall or cooled right wall on mixed convection, lid-driven flows in a square cavity. It is also observed that the average Nusselt numbers at the bottom and right walls are strong function of Grashof number at larger Prandtl numbers whereas average Nusselt number at the left wall for a specific Prandtl number is a weaker function of Grashof number. Later, Tanmay et al. [10], investigated numerically the natural convection in a trapezoidal enclosures for uniformly heated bottom wall, linearly heated vertical wall(s) in the presence of insulated top wall with a penalty finite different method for various enclosure inclination angles. An average Nusselt number plots show higher heat transfer rate for angle of inclination of  $0^\circ$  and the overall heat transfer rates at the bottom wall is larger for the linearly heated left wall and cooled right wall. Roy and Basak [11], Sathiyamoorthy et al. [12] and Natarajan et al. [13], performed a penalty finite element analysis with bi-quadratic elements. These analyses investigate uniform and non-uniform heating of wall(s) in a square enclosure, the bottom wall is uniformly heated, vertical wall(s) are linearly heated whereas the top wall is well insulated in a closed square enclosure and uniform and non-uniform heating of bottom wall in a trapezoidal enclosure on natural convection flow, respectively. The three above works were performed to investigate the influence of the boundary conditions on the forms of streamlines, isotherms contours, heat transfer rates and Nusselt numbers. Natural convection in different shapes of enclosures has also been analyzed in the presence of internal heat generation. Shim and Hyun [14] present the time dependent behavior of natural convection in a differentially heated square cavity due to impulsive switching on uniform internal heat generation. They conclude that as the transient behavior is dependent on  $Ra_E/Ra_I$ , three flow stages were distinguished. Natural convection of gas between two horizontal coaxial cylinders with uniform internal heat generation is numerically investigated by Roschina et al. [15]. It has been established that in such system there exist two types of fluid flow for low Rayleigh numbers with different vortex structure. Several special issues drew the attentions of Zhao et al. [16] on conjugate natural convection in an enclosure with external and internal

heat sources. Their analysis mainly reveals that the practices of solving the conjugate heat transfer perform well, and the sole temperature scale is flexible than the combined temperature scale for arbitrary strengths of external and internal heat sources. Oztop and Bilgen [17] and Oztop et al. [18] studied numerically the natural convection in differentially heated, partitioned and square enclosures and in a wavy-walled enclosures. They found that the flow field is modified considerably with both partial dividers and the function of wavy wall. The ratio of internal Rayleigh number to external Rayleigh number affects the heat transfer and fluid flow significantly. Measurements of the overall heat flux in steady convection have been made by Kulachi and Emara [19] in a horizontal layer of dilute aqueous electrolyte. It appears that the local temperature excesses observed in the early period of developing convection occur only for  $Ra > 100 Ra_c$ , i.e., for final steady state turbulent flow. Islam et al. [20] investigated numerically the natural convection in an inclined differentially heated square enclosure containing internally heated fluid using Galerkin finite element method. The obtained computational results indicate that the strength of the convection currents depend on the internal energy. And the heat removal rate is optimized at zero inclination angle for relatively weak external heating made for all values of internal energy. A numerical study has been made by Sivasankaran [21] to analyze the effect of thermal conductivity on the natural convection of heat generating fluids contained in a square enclosure with isothermal walls and top and bottom perfectly insulated surfaces. It is concluded that the heat transfer rate is increased by an increase in the thermal conductivity parameter. The work of Nakhi and Chamkha [22] is focused on the numerical study, laminar conjugate natural convection around a finned pipe placed in the center of a square enclosure with uniform internal heat generation. It is concluded that the maximum temperature and extreme stream function difference can be controlled through the finned pipe inclination angle and fins angle. The onset of oscillatory instability of Benard-Marangoni convection in a horizontal fluid layer subjected to the Coriolis force and internal heat generation is investigated by Char et al. [23]. The results show that smaller absolute values of critical Marangoni number and frequency take place at larger values of Cripation number. The work of Chen [24], examines the natural convection heat transfer from a horizontal isothermal cylinder of elliptic cross section in a Newtonian fluid with temperature dependent heat generation. Results show that the heat transfer rate and sink friction of the elliptical cylinder with slender orientation are higher than the elliptical cylinder with blunt orientation. Fontana et al. [25], investigated numerically the natural convection in a partially open square enclosure with internal heat source. For a low Rayleigh number, it is found that isotherm plots are smooth and follow a parabolic shape indicating the dominance of the heat source. But as the Rayleigh number increases, the flow is slowly becoming dominant by the temperature difference by the walls. An analysis of Higuera and Ryazantsev [26] presented the laminar natural convection flow due to localized heat source on the center line of a long vertical channel or pipe whose wall is kept at a constant temperature. It is found that the optimal height of the channel is leading to maximum mass flux and minimum temperature for a given heat released rate. Deshmuch et al. [27] investigated natural convection circulation in enclosures with uniform heat generation for different Prandtl number fluids. It is found that the steady state solutions are obtained for all Rayleigh number, except at Rayleigh number=10<sup>6</sup>. Natural convection flow from a horizontal circular cylinder with uniform heat flux in presence of heat generation has been investigated by Molla et al. [28]. It is clear from the results that the pressure distribution increases was increasing heat generation. Recently, Hussein and Hussain [29] studied numerically the problem of two-dimensional laminar natural convection in a tilted square enclosure in the presence of internal heat generation using finite volume method. The results indicate that as the inclination angle increases, the hydrodynamic boundary layer at the hot and cold sidewalls decreases. On the other hand, the thermal boundary layers increases as the internal heat source increases.

From the literature review cited above it can be seen numerous numerical and experimental researches have studied the steady laminar natural convection of the fluid medium in differently shaped enclosures in the presence or absence of internal heat generation or uniformly and non-uniformly heated sidewalls, but the best part of this paper which is to study the natural convection inside parallelogram shaped enclosure including internal heat generation and linearly heated wall boundary has not been addressed yet; therefore, in this study we investigate these objectives. The numerical results have been solved by using finite volume method. The governing parameters studied are ( $\Phi$ ) angle of inclination, internal Rayleigh number ( $Ra_i$ ) and external Rayleigh number ( $Ra_e$ ).

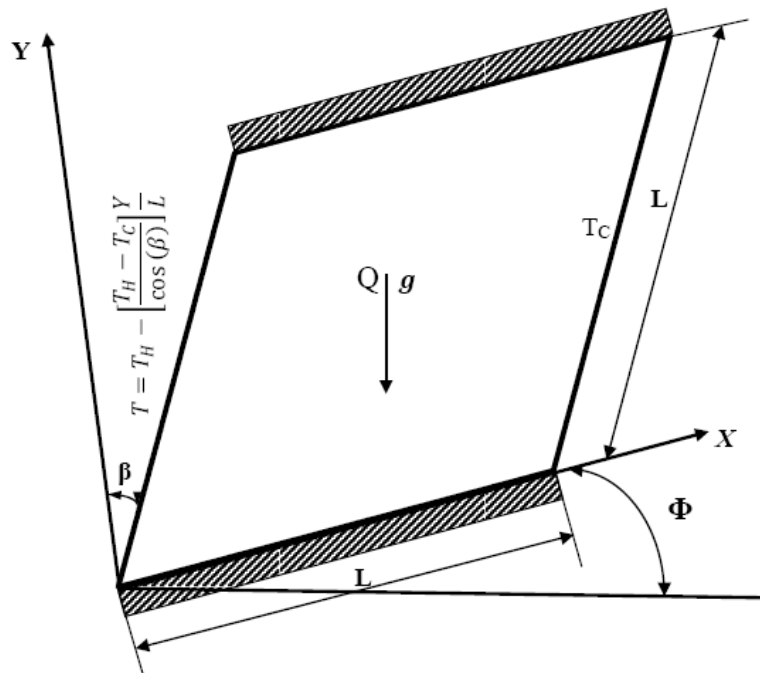


Fig. 1. Schematic diagram and coordinate system of the physical domain with boundary conditions

## 2. Mathematical analysis

The geometry and coordinate system of the problem under consideration is described in Fig. 1. It consists of a parallelogram-shaped enclosure of dimension,  $L$ , whose both left and right walls are isothermal but temperature of left wall is higher than that of right wall which is inclined at an angle ( $\beta = 30^\circ$ ) with respect to vertical. However, the upper and lower walls are considered to be thermally insulated. The enclosure is filled with an air whose its Prandtl number is taken as 0.71. The enclosure under investigation is inclined at inclination angles of ( $\Phi$ ) ranging from  $0^\circ$  to  $45^\circ$ . All the numerical calculations are performed at the external Rayleigh numbers ranging from  $10^3$  to  $10^6$  while the internal Rayleigh numbers ranges from  $10^5$  to  $10^8$ . The solution is obtained by using a finite volume scheme and the following assumptions are considered in the present analysis :

1. The flow is considered laminar, steady and two dimensional.
2. The fluid properties are assumed constant except for the density variation in the buoyancy term which is treated according to Boussinesq approximation.
3. The fluid inside the enclosure is assumed Newtonian and incompressible while viscous dissipation effects are considered negligible.
4. The model is assumed not to be subjected to any external flow; hence the internal natural convection phenomenon is studied for the present model.

The laminar internal two-dimensional flow and the temperature distribution inside the enclosure are described by the Navier–Stokes and the energy equations, respectively. The governing equations are transformed into dimensionless forms by using the following dimensionless variables[20];

$$\theta = \frac{T - T_c}{T_h - T_c}, X = \frac{x}{L}, Y = \frac{y}{L}, U = \frac{uL}{\vartheta}, V = \frac{vL}{\vartheta}, \text{ and } P = \frac{pL^2}{\rho\vartheta^2} \quad (1)$$

The dimensionless forms of the governing equations are expressed in the following forms [20];

$$\frac{\partial U}{\partial X} + \frac{\partial V}{\partial Y} = 0 \quad (2 - a)$$

$$U \frac{\partial U}{\partial X} + V \frac{\partial U}{\partial Y} = -\frac{\partial P}{\partial X} + \left( \frac{\partial^2 U}{\partial X^2} + \frac{\partial^2 U}{\partial Y^2} \right) + \left( \frac{Ra_E}{Pr} \sin \Phi \right) \theta \quad (2 - b)$$

$$U \frac{\partial V}{\partial X} + V \frac{\partial V}{\partial Y} = -\frac{\partial P}{\partial Y} + \left( \frac{\partial^2 V}{\partial X^2} + \frac{\partial^2 V}{\partial Y^2} \right) + \left( \frac{Ra_E}{Pr} \cos \Phi \right) \theta \quad (2 - c)$$

$$U \frac{\partial \theta}{\partial X} + V \frac{\partial \theta}{\partial Y} = \frac{1}{Pr} \left( \frac{\partial^2 \theta}{\partial X^2} + \frac{\partial^2 \theta}{\partial Y^2} \right) + \left( \frac{Ra_I}{Ra_E Pr} \right) \quad (2-d)$$

where  $Ra_E$  is the external Rayleigh number and  $Ra_I$  is the internal Rayleigh number. The previous dimensionless numbers are defined by [30] as;

$$Pr = \frac{\vartheta}{\alpha}, \quad Ra_E = \frac{g \gamma (T_h - T_c) L^3 Pr}{\vartheta^2} \quad \text{and} \quad Ra_I = \frac{g \gamma G L^5}{\vartheta k \alpha} \quad (3)$$

where  $\gamma$  is the volumetric coefficient of thermal expansion,  $\vartheta$  is the kinematic viscosity,  $\alpha$  is the thermal diffusivity and  $g$  is the gravitational acceleration. Two types of Rayleigh number are defined in this work, the first is called internal Rayleigh number ( $Ra_I$ ), which represents the strength of the internal heat generation and the other is called external Rayleigh number ( $Ra_E$ ), which represents the effect due to the differential heating of the isothermal sidewalls. The rate of heat transfer is expressed in terms of average Nusselt number ( $\overline{Nu}$ ) as follows;

$$\overline{Nu} = - \int_0^1 \left[ \frac{\partial \theta}{\partial X} \right]_{X=0} dy \quad (4)$$

### 3. Boundary conditions

The boundary conditions which are used in the present study can be arranged as follows;

1. The top wall is thermally insulated, so;

$$\frac{\partial \theta}{\partial y} = 0, \quad U = V = 0 \quad (5)$$

2. The bottom wall is thermally insulated, so;

$$\frac{\partial \theta}{\partial Y} = 0, \quad U = V = 0 \quad (6)$$

3. The left side wall is linearly heated, so;

$$\theta = 1 - Y / \cos(30^\circ), \quad U = V = 0 \quad (7)$$

4. The right side wall is kept at a uniform cold temperature, so;

$$\theta = 0 \quad \text{and} \quad U = V = 0 \quad (8)$$

### 4. Numerical solution procedure

Firstly the problem is defined as a steady, laminar, and two dimensional parallelogram-shaped enclosure. Control volume based on Finite Volume Method (FVM) is to be used to discretize the governing differential flow equations as discussed by Patankar [31]. Central differencing is used to discretize the diffusion terms, whereas a blending of upwind and central differencing is used for the convection terms. Computing the collocated grid requires computing the cell face velocities. The pressure- velocity coupling in the governing equations is achieved using the well-known SIMPLE algorithm for numerical computations. The pressure correction equation is derived from the continuity equation to enforce the local mass balance as given in Ferziger and Peric [32]. Linear interpolation and numerical differentiation are used to express the cell-face value of the variables and their derivatives through the nodal values. The final discretized form of governing equations is to be solved sequentially using the Strongly Implicit Procedure (SIP) solver [33]. Iteration is continued until difference between two consecutive field values of variable is less than or equal to  $10^{-6}$ . Further stabilities of numerical algorithm, under relaxation factors of 0.2-0.85 are used in the present computations. The description of this solution method is given very well in Ferziger and Peric [32] and the details are not given here for brevity.

### 5. Grid refinement check

Two dimensional body fitting grids used for the present computation. The 2-D computational grids are clustered towards the walls. The location of the nodes is calculated using a stretching function as described by Thompson et al. [34] so that the node density is higher near the walls and the round corners of the parallelogram-shaped enclosure. In order to obtain grid independent solution, a grid refinement study is performed for the configuration problem of the present study with  $Ra_E = 10^6$ ,  $Ra_I = 10^8$ ,  $Pr = 0.71$ , and  $\Phi = 45^\circ$ . In the present work, eight combinations (40 x 40, 50 x 50, 60 x 60, 70 x 70, 80 x 80, 100 x 100, 120 x 120 and 150 x 150) of non-uniform grids are used to test the effect of grid size on the accuracy of the predicted results. Fig. 2 shows the convergence of the average Nusselt number ( $\overline{Nu}$ ), at the linearly heated sidewall of the parallelogram-shaped enclosure with grid refinement. It is observed that grid independence is achieved with combination of (120x120) control volumes where there is insignificant change in the average Nusselt number ( $\overline{Nu}$ ) with the improvement in finer grid. The agreement is found to be excellent which validates the present computations indirectly.

## 6. Numerical results verification

For the purpose of the present numerical algorithm verification, a laminar natural convection problem is investigated in which square cavity is filled with air ( $Pr = 0.71$ ) with horizontal walls assumed adiabatic, while the sidewalls are isothermal but kept at different temperatures, containing internal energy source. A  $120 \times 120$  mesh with clustering towards the walls is used and computations are done for  $Ra_E = 10^5$ ,  $Ra_I = 10^7$ . Comparisons of the average Nusselt numbers at uniformly heated left sidewall are shown in Table 1.

The general agreement between the present computation and the previous values obtained by Tofiqul et al. [20] is seen to be very well with a maximum deviation of about 6.478%. Further verification is performed by using the present numerical algorithm to investigate the same problem considered by Tofiqul et al. [20] and Shim and Hyun [14] using the same flow conditions, geometries and the boundary conditions but the numerical scheme is different. The comparison is made using the following dimensionless parameters:  $Pr = 0.71$ ,  $Ra_E = 10^5$ ,  $Ra_I = 10^7$  and  $\Phi = 0^\circ$ . Excellent agreement is achieved between the results of Tofiqul et al. [20] and Shim and Hyun [14] and the present numerical scheme results for both streamlines and temperature contours inside the square cavity filled with air as shown in Fig. 3. These verifications give a good confidence in the present numerical model to deal with the physical problem.

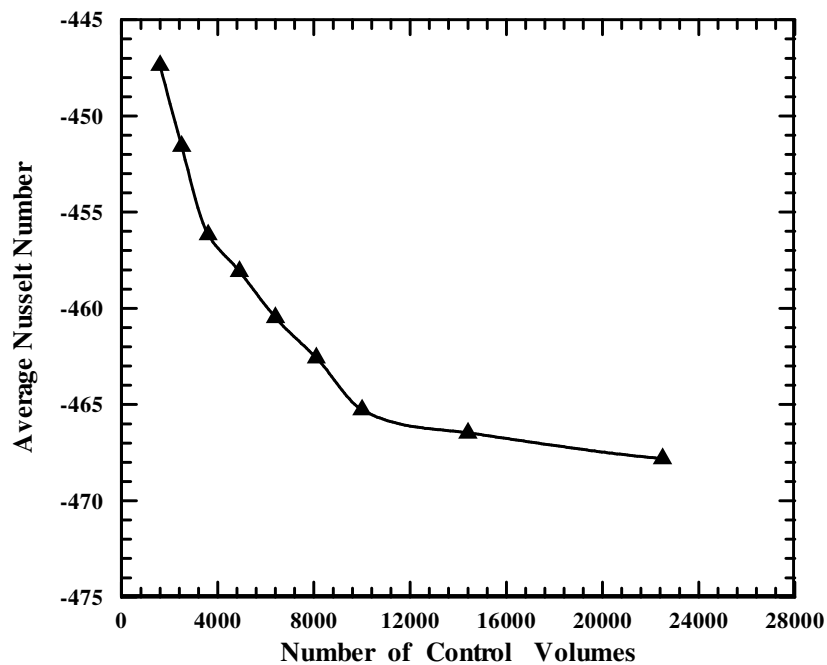


**Fig. 2.** Convergence of average Nusselt number along the linearly heated side wall of the parallelogram-shaped enclosure with grid refinement at  $Ra_E = 10^6$ ,  $Ra_I = 10^8$ ,  $Pr = 0.71$  and  $\Phi = 45^\circ$ .

## 7. Results and discussion

The objective of this paper is to study the flow field and isotherms inside an inclined parallelogram-shaped enclosure and the average Nusselt number distribution along linear side wall with external Rayleigh number ( $Ra_E$ ) ranging from  $10^3$  to  $10^6$ , internal Rayleigh number ( $Ra_I$ ) ranging from 0 to  $10^8$  and enclosure inclination angle ( $\Phi$ ) ranging from  $0^\circ$  to  $45^\circ$ . Air is chosen as a working fluid with  $Pr = 0.71$ .

**Table 1**

Comparison of the present average Nusselt number along the heated left side wall with those of previous studies.

$Ra_I$	$Ra_E$	$\bar{Nu}$			Maximum deviation %
		Shim and Hyun [14]	Tofiqul et al. [20]	present work	
$10^6$	$10^5$	-0.1	-0.1	-0.100125	0.125
$10^7$	$10^5$	-46.0	-43.02	-43.01985	6.478

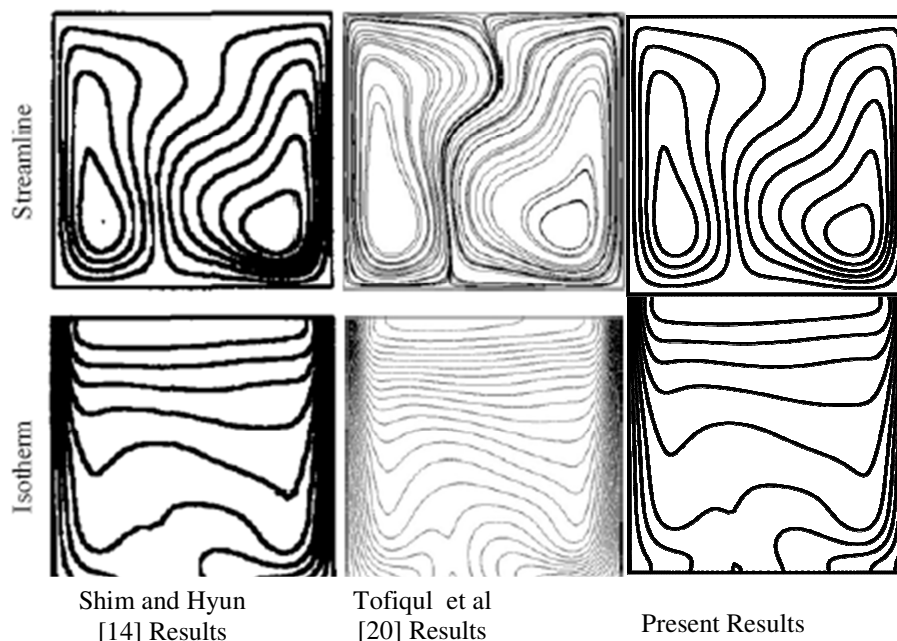


**Fig. 3.** Comparison of streamlines and isotherms between the results of the present work and that of Shim and Hyun [14] and Tofiqul et al [20] in the square cavity filled with air using flow conditions ( $Pr = 0.71$ ,  $Ra_E = 10^5$ ,  $Ra_I = 10^7$ ,  $\Phi = 0^\circ$ ).

### 7-1. Flow- thermal structure

The flow structures and the thermal field are presented by the streamlines and isotherms in Figs. 4 and 5, respectively, for  $Ra_E = 10^3$  and all values of  $Ra_I$  and  $\Phi$ . It can be seen from Fig. 4 for streamlines distribution at  $Ra_I = 0$  (non-heat generation) and  $\Phi = 0^\circ$ , the enclosure is occupied by a single large clockwise vortex centered in the main enclosure, with intense upward and downward flows adjacent to the left hot wall and to the right cold wall, respectively. When the inclination angle is increased  $\Phi > 0^\circ$ , the intensity of the circulation is increased and hence, the maximum value of stream function is observed and the streamlines are distributed uniformly. But no significant changes in the flow characteristics are noted. With a Rayleigh number of  $10^5 \geq Ra_I \geq 10^6$  and  $\Phi = 0^\circ$ , the enclosure is filled by two vortices due to opposing and aiding buoyancy force. Both counter-clockwise and clockwise vortices near the hot and cold side walls, respectively. Furthermore an increase in Rayleigh number range from  $10^7 \geq Ra_I \geq 10^8$  and  $\Phi = 0^\circ$ , indicating that the flow pattern is influenced greatly by heat source than the temperature difference. Hence, the streamlines are distorted due to vigorous sinking motion and the heat transfer rate is enhanced.

With the increasing of enclosure inclination angle ( $\Phi > 0^\circ$ ), the flow patterns are clustered and compressed towards the sidewalls forming a thick boundary layer, due to x-component of buoyancy force and the external heating oppose the flow of the two vortices. Moreover, the right cold vortex begins to enlarge while the left hot vortex begins to decrease. As well as, the cores of the left and right vortices move down toward the left and right bottom corners respectively. The results when  $Ra_E = 10^3$  indicate that the flow field resulting from the internal heat source has a greatest effect than the flow field resulting from the differentially heated sidewalls of the enclosure due to buoyancy force effect.

Fig. 5 illustrates isotherms for  $Ra_E = 10^3$ . As expected from the streamlines contours in Fig. 4 at  $Ra_I = 0$  where no significant changes in the flow characteristics are noticed with the increasing of the enclosure inclination angle. With the same increasing of the enclosure inclination angle ( $\Phi$ ) at  $Ra_I = 0$  in Fig. 5, the isotherms don't change dramatically and the convection is the basic mode. And when  $Ra_I = 10^5$ , the distribution of the isotherms basically implies that the enclosure is in natural convection domain. As  $10^6 \geq Ra_I \geq 10^8$ , the isotherms at the upper core portion of the enclosure are almost distributed linearly (horizontally and vertically one to each other) showing conduction dominant heat transfer begins to be observed at this portion. But at the lower part of the enclosure the convection heat transfer regime is remaining dominant.

Generally, when the enclosure inclination angle ( $\Phi$ ) is increased, then the circulation motion is enhanced

and when  $Ra_I \geq 10^5$  the isotherms lines indicate that the enclosure becomes similar to that of pure convection. But when  $10^6 \geq Ra_I \geq 10^8$  the isotherms lines indicate that the enclosure becomes similar to that of pure conduction at the upper part and convection at the others. Similarly when the two cores of the streamlines vortices move downward to the lower portion of the enclosure, see Fig. 4, the isotherms forming two groups too, as shown in Fig. 5. It is also interesting to observe that as internal heat generation increases the isotherms compressed to the sidewalls then the discrete isotherms near the sidewalls get compressed strongly towards the sidewalls due to high temperature gradient within the thermal boundary layer. The thermal boundary layers near the left heated sidewall and the right cold sidewall increases from bottom to upper as the effect of the internal heat generation increases. As the external Rayleigh number increases to  $10^6$ , Figs. 6 and 7 show the streamlines and isotherms contours. In fact, the action of  $Ra_E$  is completely clear in this case. Generally, the distortion of the streamlines started earlier in this case of  $Ra_I = 0$  if it is compared with the same previous case of  $Ra_E = 10^3$ . This is due to chaotic flow and earlier increasing in the linearly heating of the left sidewall with increasing of  $Ra_E$  to  $10^6$ , then the better energy transfer is done by convection here. It is obvious from the streamlines contour of  $Ra_E = 10^6$ , Fig. 6, when  $Ra_I \leq 10^6$  and  $\Phi = 0^\circ$ , the enclosure is occupied by a large dominate clockwise vortex fill almost the area of the enclosure and another very weak and small vortex at the upper left corner of the enclosure. Instantaneously, the effect of external heating is greater than the effect of internal heating, and then the convection heat transfer is still dominated. As a result of increasing of enclosure inclination angle ( $\Phi$ ), the circulation becomes stronger, more uniform and smoother. Some perturbation can be noted in the upper right and lower left corners due to impingement of the fluid to the side walls, and some small and weak vortices appear and vanish in the core of the enclosure.

An increase in Rayleigh number  $Ra_I \geq 10^7$  provides an equal heat generation effect on left hot and right cold sides, the circulation becomes intensive especially near the hot wall side, and the high heat generation rate produced two opposite directions, irregular and differs in intensity vortices. I.e., aiding buoyancy force on the left vortex and opposing buoyancy force on the right vortex. Hence, the weak and small vortex at the upper left corner begins to expand. With increasing in the enclosure inclination angle ( $\Phi$ ), the right cold vortex begin to expand and press and lift the left small and hot vortex to the upper left corner at  $Ra_I = 10^7$  and to the left hot side wall at  $Ra_I = 10^8$ . An increasing in the enclosure inclination angle ( $\Phi$ ) implies that the heat transfer by convection is dominated and forming a complex expected streamlines. It is very important to observed that at  $Ra_I = 0$  and  $\Phi = 0^\circ$ , the same dominated vortex that seen in the streamlines of Fig. 6 is found here in Fig. 7 but in isotherms form. As  $Ra_I = 0$  and  $\Phi = 0^\circ$ , no heat generation inside the enclosure, the flow is controlled by the temperature difference of hot and cold side walls only then the convection heat transfer is domineer here. Further increase in Rayleigh number to  $10^6$  and  $\Phi = 0^\circ$ , the rate of heat generation increases gradually, then the isotherms curves started to change its shape to the linear forms indicating that the conduction heat transfer starts to be dominant at the upper part of the enclosure. But at the lower part of the enclosure the convection heat transfer regime is remaining dominant. It can be noticed from the results Fig. 7, when the internal heat generation increases, the thermal boundary layers begin to increase adjacent to the hot and cold sidewalls.

As mentioned before, when the enclosure inclination angle ( $\Phi$ ) is increase and  $Ra_I \leq 10^6$  the circulation motion is enhanced and the isotherms indicate that the enclosure becomes similar to that of pure convection. when the enclosure inclination angle ( $\Phi$ ) is increase and  $10^7 \geq Ra_I \geq 10^8$ , the shape of the isotherms don't change so much implying that the diagonally linear isotherms in a conduction mode form at the upper part and convection mode form at the lower part of the enclosure.

## 7-2. Heat transfer characteristics

Average Nusselt number on the linearly heated wall calculated by Eq. (4) is presented in Fig. 8, as a function of the internal heat generation,  $Ra_I$  from  $10^5$  to  $10^8$  for different inclination angles and for different external heating of  $Ra_E = 10^3$  to  $Ra_E = 10^6$ . The results show that the average Nusselt number remains invariant between the  $Ra_I = 10^5$  to  $Ra_I = 10^6$  but it increases rapidly when internal heat generation increases above this range because of the impact of internal heat generation. Maximum average Nusselt number is obtained for minimum value of external heating ( $Ra_E = 10^3$ ) and for  $\Phi = 0^\circ$  for all values of  $Ra_E$ , because of high convective heat transfer. The negative sign of Nusselt number values means that the linearly heated wall receives the heat from the inside hot fluid.

## 8. Conclusions

Natural convection in a tilted parallelogram-shaped enclosure having linearly heated wall (left sidewall) and cold wall (right sidewall) while the horizontal walls are well insulated and contain internal heat generation is studied numerically. The governing equations for this study are put in the dimensionless forms and are solved by using finite volume technique. Results are presented in streamlines and isotherms for all parametric studies. From the results presented above, the main conclusions are as follows;

1. The isotherms lines become more vigorous at high external heating ( $Ra_E = 10^6$ ) and convection heat transfer represents the principal mode.

2. Maximum Nusselt number is obtained when the relatively weak external heating ( $Ra_E=10^3$ ) and high internal heat generation ( $Ra_I=10^8$ ) and angle of inclination  $\Phi=0^\circ$ , see Fig. 8a.
3. An increase in  $Ra_I$  leads to an increase in the values of streamlines, temperature gradient and thickness of the boundary layer.
4. When  $Ra_E=10^3$  and  $Ra_I > 0$ , the enclosure is occupied by two circulations, i.e, both anti-clockwise and clockwise vortices near the hot and cold side walls due to negative and positive buoyancy effect respectively.
5. The circulation near the heated wall is less intense than the main circulation; the heat generation begins to lose its importance to the difference in temperature between the wall sides at high  $Ra_E=10^6$ .
6. The flow and the heat transfer are controlled by the internal heat generation and difference in temperatures of sides walls.
7. When  $Ra_E=10^3$  the isotherms can be controlled mainly by the heat source ( $Ra_I$ ), then the conduction heat transfer is very clear to be dominant. Vice versa, and controlled by temperature difference ( $Ra_E$ ) when  $Ra_E=10^6$ , then the convection heat transfer is very clear to be dominant.
8. Due to different buoyancy forces effect on the left and right vortices, the circulation close to cold side wall is greater than that close to right hot side wall.
9. At  $\Phi=0^\circ$  and  $Ra_E=10^3$  the two vortices is appeared at  $Ra_I=10^5$ , but at  $Ra_E=10^6$  the two vortices is appeared at  $Ra_I=10^7$ , this make to understand that the conduction is dominant at lowest Rayleigh number and the convection is dominant at the highest Rayleigh number.

### Nomenclature

$g$	Gravitational acceleration, ( m/s <sup>2</sup> )
$G$	Uniform volumetric heat generation (W/m <sup>3</sup> )
$k$	Thermal conductivity of fluid, (W / m.°C)
$L$	Length or width of the enclosure (m)
$\overline{Nu}$	Average Nusselt number
$P$	Dimensionless pressure
$p$	Pressure, (N/m <sup>2</sup> )
$Pr$	Prandtl number
$Ra_E$	External Rayleigh number
$Ra_I$	Internal Rayleigh number
$T$	Temperature, (°C)
$T_c$	Temperature of the cold surface, (°C)
$T_h$	Temperature of the hot surface, (°C)
$U$	Dimensionless velocity component in x-direction
$u$	Velocity component in x-direction, (m/s)
$V$	Dimensionless velocity component in y-direction
$v$	Velocity component in y-direction, (m/s)
$W$	Width of the flat bottom of the enclosure,(m)
$X$	Dimensionless coordinate in horizontal direction
$x$	Cartesian coordinate in horizontal direction, (m)
$Y$	Dimensionless coordinate in vertical direction
$y$	Cartesian coordinate in vertical direction, (m)

### Greek symbols

$\alpha$	Thermal diffusivity, (m <sup>2</sup> /s)
$\gamma$	Volumetric coefficient of thermal expansion, (K <sup>-1</sup> )
$\beta$	Sidewall enclosure inclination angle from vertical direction, (degree)
$\Phi$	Enclosure inclination angle with horizontal direction, (degree)
$\theta$	Dimensionless temperature
$\rho$	Density of the fluid, (kg/m <sup>3</sup> )
$\vartheta$	Kinematic viscosity of the fluid, (m <sup>2</sup> /s)

### References

- [1] Nakamura H, Asako Y. Heat transfer in a parallelogram shaped enclosure, Bulletin of the JSME 1980;4:1827-1834.
- [2] Asako Y, Nakamura H. Heat transfer in a parallelogram shaped enclosure, Bulletin of the JSME 1982;



25:1412-1418.

- [3] Asako Y, and Nakamura H. Heat transfer in a parallelogram shaped enclosure, *Bulletin of the JSME* 1984; 27:1144-1151.
- [4] Naylor D, Oosthuizen P H. A numerical study of free convective heat transfer in a parallelogram-shaped enclosure. *Int. J. Num. Heat Fluid Flow* 1994; 4:553-559.
- [5] Costa V A F. Double-diffusive natural convection in parallelogramic enclosure filled with fluid saturated porous media. *Int. J. Heat and Mass Transfer* 2004; 47: 2699-2714.
- [6] Costa V A F, Oliveira M S A, Sousa A C M. Laminar natural convection in a vertical stack of parallelogramic partial enclosures with variable geometry. *Int. J. Heat and Mass Transfer* 2005; 48: 779-792.
- [7] Bairi A, Garcia de Maria J M, Laraqi N. Transient natural convection in parallelogramic enclosure with isothermal hot wall. Experimental and numerical study applied to on-board electronics. *Applied Thermal Energy* 2010; 30:1115-1125.
- [8] Maria J M G D, Bairi A, Costa V A F. Empirical correlation at high Ra for steady-state free convection in 2D air-filled parallelogramic enclosures with isothermal discrete heat sources. *Int. J. of Heat and Mass Transfer* 2010; 53:3831-3838.
- [9] Tanmay Basak, Roy S, Pawan Kumar Sharma, Pop I. Analysis of mixed convection flows within a square cavity with linearly heated side wall(s). *Int. J. of Heat and Mass Transfer* 2009; 52:2224-2242.
- [10] Tanmay Basak, Roy S, Amit Singh, Bishun D P. Natural convection flow simulation for various angles in a trapezoidal enclosure with linearly heated side wall(s). *Int. J. of Heat and Mass Transfer* 2009; 52: 4413-4425.
- [11] Roy S, Tanmay Basak, Finite element analysis of natural convection flows in a square cavity with non-uniform heated wall(s). *Int. J. of Engineering Science* 2005; 43:668-680.
- [12] Sathiyamoorthy M, Tanmay Basak, Roy S, Pop I. Steady natural convection flow in a square cavity filled with a porous medium for linearly heated side wall(s). *Int. J. of Heat and Mass Transfer* 2007; 50:1892-1901.
- [13] Natarajan E, Tanmay Basak, Roy S, Natural convection flows in a trapezoidal enclosure with uniform and non-uniform heating of bottom wall. *Int. J. of Heat and Mass Transfer* 2008; 51:747-756.
- [14] Shim Y M, Hyun J M. Transient confined natural convection with internal heat generation. *Int. J. Heat Fluid Flow* 1997; 18: 328-333.
- [15] Roschina N A, Uvarov A V, Osipov A I. Natural convection in an annulus between coaxial horizontal cylinders with internal heat generation. *Int. J. of Heat and Mass Transfer* 2005; 48: 4518-4525.
- [16] Zhao F Y, Guang-Fa Tang, Di Liu. Conjugate natural convection in enclosures with external and internal heat sources. *Int. J. of Engineering Science* 2006; 44:148-165.
- [17] Oztop H, Bilgen E. Natural convection in differentially heated and partially divided square cavities with internal heat generation. *Int. J. Heat Fluid Flow* 2006; 27: 466-475.
- [18] Oztop H, Abu-Nada E, Varol Y, and Chamkha A. Natural convection in a wavy enclosures with volumetric heat sources. *Int. J. of Thermal Sciences* 2011; 50: 502-514.
- [19] Kulachi F A, Emara A A. Steady and transient thermal convection in a fluid layer with uniform volumetric energy sources. *J. Fluid Mechanics* 1977; 83:375-395.
- [20] Tofiqul Islam, Sumon Saha, Arif Hasan Mamun. Natural convection in an inclined square enclosure containing internal energy sources. *The Institution of Engineers, Bangladesh. J. Mech. Eng.* 2007; 37:24-32.
- [21] Sivasankaran S. Effect of variable thermal conductivity on buoyant convection in a cavity with internal heat generation. *Nonlinear Analysis: Modeling and Control* 2007; 12: 113-122.
- [22] Ben-Nakhi Abdullatif, Chamkha Ali J. Conjugate natural convection around a finned pipe in a square enclosure with internal heat generation. *Int. J. of Heat and Mass Transfer* 2007; 50: 2260-2271.
- [23] Char M, Chiang K T, Jou J J. Oscillatory instability analysis of Benard-Marangoni convection in a rotating fluid with internal heat generation. *Int. J. of Heat and Mass Transfer* 1997; 40: 857-867.
- [24] Ching-Yang Cheng. Natural convection heat transfer from a horizontal isothermal elliptical cylinder with internal heat generation. *Int. Comm. Int. Heat and Mass Transfer* 2009; 36: 346-350.
- [25] Fontana E, Silva A D, Mariani V C. Natural convection in a partially open square cavity with internal heat source: An analysis of the opening mass flow. *Int. Heat and Mass Transfer* 2011; 54: 1369-1386.
- [26] Higuera F J, Ryazantsev Y S. Natural convection flow due to a heat source in a vertical channel. *Int. Heat and Mass Transfer* 2002; 45: 2207-2212.
- [27] Deshmukh P, Mitra S K, Gaitonde U N. Investigation of natural circulation in cavities with uniform heat generation for different Prandtl number fluids. *Int. Heat and Mass Transfer* 2011; 54: 1465-1474.
- [28] Molla M M, Paul S C, Hossain M A. Natural convection flow from a horizontal circular cylinder with uniform heat flux in presence of heat generation. *Applied Mathematical Modeling* 2009; 33:3226-3236.
- [29] Hussein A K, Hussain S H. Numerical analysis of steady natural convection of water in inclined square enclosure with internal heat generation, *International Conference on Mechanical and Electrical Technology (ICMET)*, 10-12 September, Singapore, 2010.
- [30] Arpaci P, Larsen P, *Convection Heat Transfer*, Prentice-Hall, 1984.

- 
- [31] PatankarSV.Numerical heat transfer and fluid flow. Hemisphere Publishing Corporation, New York,1980.  
[32] FerzigerJ, PericM. Computational methods for fluid dynamics, 2nd edition Springer, New York,1999.  
[33] StoneHL.Iterative solution of implicit approximations of multidimensional partial differential equations. SIAM J. Numer. Anal. 1968;5: 530–558.  
[34] Thompson PD,ThamasFC,Mastin F.Automatic numerical generation of body- fitted curvilinear coordinate system. J. of Computational Physics1974;15:299-319.

The IISTE is a pioneer in the Open-Access hosting service and academic event management. The aim of the firm is Accelerating Global Knowledge Sharing.

More information about the firm can be found on the homepage:

<http://www.iiste.org>

### CALL FOR JOURNAL PAPERS

There are more than 30 peer-reviewed academic journals hosted under the hosting platform.

**Prospective authors of journals can find the submission instruction on the following page:** <http://www.iiste.org/journals/> All the journals articles are available online to the readers all over the world without financial, legal, or technical barriers other than those inseparable from gaining access to the internet itself. Paper version of the journals is also available upon request of readers and authors.

### MORE RESOURCES

Book publication information: <http://www.iiste.org/book/>

Academic conference: <http://www.iiste.org/conference/upcoming-conferences-call-for-paper/>

### IISTE Knowledge Sharing Partners

EBSCO, Index Copernicus, Ulrich's Periodicals Directory, JournalTOCS, PKP Open Archives Harvester, Bielefeld Academic Search Engine, Elektronische Zeitschriftenbibliothek EZB, Open J-Gate, OCLC WorldCat, Universe Digital Library, NewJour, Google Scholar

